Journal of Applied Pharmaceutical Research
Volume 14 Issue 3, Year of Publication 2026, Page 177 – 191
DOI: https://doi.org/10.69857/joapr.v14i3.2008

Check for updates

Research Article

JOURNAL OF APPLIED PHARMACEUTICAL RESEARCH | JOAPR
www.japtronline.com ***ISSN: 2348 – 0335***

QUINOXALINE AMINO DERIVATIVES AS POTENTIAL EGFR-TARGETED THERAPEUTICS IN BREAST CANCER: COMPUTATIONAL EXPLORATION

Abitha H[1,2], D. Kumudha[1*], Bhuvaneswari Sivaraman[3], M. K. Kathiravan[4]

Article Information
Received: 31st December 2025
Revised: 17th March 2026
Accepted: 24th April 2026
Published: 15th May 2026

Keywords
EGFR, ADMET, TNBC, MMGBSA, Breast cancer, Quinoxaline amino derivatives.

ABSTRACT

Background: Despite resistance to current tyrosine kinase inhibitors, which makes the epidermal growth factor receptor (EGFR) a recognized therapeutic target in breast cancer, there is a need for novel inhibitors. Quinoxaline compounds are a promising scaffold for next-generation EGFR inhibitors and exhibit favorable pharmacological properties. **Methodology:** Ten new amino quinoxaline derivatives (QN1–QN10) were systematically developed and assessed by a comprehensive in silico approach. Molecular docking was conducted on the EGFR tyrosine kinase domain (PDB ID: 4HJO) utilizing Glide XP, with erlotinib serving as the reference ligand. Drug-likeness, oral bioavailability, and synthetic accessibility were evaluated using SwissADME, whereas pkCSM predicted ADMET characteristics. The most effective candidate was subsequently corroborated by 100 ns molecular dynamics (MD) simulations utilizing GROMACS 2021.1, succeeded by MM-GBSA binding free energy assessments. **Results and Discussion**: According to docking data, QN8 proved the most promising inhibitor. It showed stable hydrogen bonding with key EGFR hinge residues (MET769 and ASP831) and a high binding affinity (−9.305 kcal/mol), comparable to erlotinib (−9.501 kcal/mol). Consistent RMSD and RMSF profiles from MD simulations corroborated the structural stability of the QN8–EGFR complex. According to MM-GBSA analysis, the van der Waals, lipophilic, and electrostatic contributions were the main drivers of the favorable binding free energy (-73.63 kcal/mol). Pharmacokinetic predictions showed adequate ADMET properties and good oral absorption. **Conclusion:** This exhaustive computational analysis highlights amino quinoxaline derivatives as promising leads for developing breast cancer drugs, identifying QN8 as a strong EGFR inhibitor with stable binding dynamics and favorable drug-like properties.

[1]*Faculty of Pharmacy, Karpagam Academy of Higher Education, Coimbatore-641021, Tamil Nadu, India.*
[2]*Department of Pharmaceutical Chemistry, Nehru College of Pharmacy, Thrissur-680588, Kerala, India.*
[3]*Department of Pharmaceutical Chemistry, SRM College of Pharmacy, Faculty of Medicine and Health Sciences, SRM Institute of Science and Technology, Kattankulathur 603203, Chengalpattu District, Tamil Nadu, India.*
[4]*Dr APJ Abdul Kalam Research Laboratory, SRM College of Pharmacy, Faculty of Medicine and Health Sciences, SRM Institute of Science and Technology, Kattankulathur 603203, Chengalpattu District, Tamil Nadu, India.*

For Correspondence: **drkumudha.d@kahedu.in**

INTRODUCTION

Cancers of the breast and lung have emerged as societal issues that have a significant financial impact worldwide, particularly in low- and middle-income nations. The unregulated development and spread of abnormal cells are hallmarks of cancer, an elaborate and diverse condition [1]. About 10–20% of all instances of breast cancer worldwide are Triple-Negative Breast Cancer (TNBC), a particularly aggressive and complex form of malignancy. This subtype of breast cancer is differentiated from other subtypes by being devoid of expression of the human epidermal growth factor receptor 2 (HER2), progesterone receptors (PR), and estrogen receptors (ER).

The administration of hormonal therapies or HER2-targeted interventions, like trastuzumab or tamoxifen, which are highly efficient in treating other forms of breast cancer, is restricted by the absence of these crucial receptors. Since chemotherapy has been connected with elevated instances of recurrent cancers and resistance to therapies, individuals with TNBC generally have a handful of treatment options. TNBC is the primary focus of research efforts owing to its aggressive clinical features and lack of specific medications, thereby driving the development of more individualized and effective treatments [2, 3].

Clinically approved EGFR tyrosine kinase inhibitors (TKIs), including first-generation reversible inhibitors such as Gefitinib and Erlotinib, and second-generation inhibitors like Lapatinib, have demonstrated therapeutic efficacy in malignancies. However, their long-term clinical utility is severely limited by the emergence of acquired resistance. One of the most significant reasons for resistance is the T790 M mutation at the gatekeeper residue, which reduces inhibitor binding affinity through steric hindrance and increased ATP affinity. Though third-generation inhibitors slightly overcome resistance, they show off-target toxicities.

Quinoxaline-based amino derivatives represent a promising scaffold for EGFR inhibition. Unlike classical quinazoline-based TKIs, quinoxaline scaffolds possess a rigid heteroaromatic moiety with favorable electronic properties for flexible substitution that can access both the ATP-binding cleft and adjacent hydrophobic pockets of the EGFR kinase domain. This helps facilitate interactions via hydrogen bonding and hydrophobic interactions beyond the conserved hinge region, reducing sensitivity to mutations such as T790M. Moreover, the presence of amino substituents on the quinoxaline core enhances binding adaptability and facilitates interactions that are less dependent on residues commonly altered during resistance development. The exploration of quinoxaline amino derivatives is justified as a strategic approach to overcome known resistance mechanisms, providing a strong structural and mechanistic basis for the development of next-generation EGFR-targeted therapeutics.

The triple-negative breast cancer (TNBC) is heterogeneous; a substantial subset of TNBC tumors exhibits marked overexpression of epidermal growth factor receptor (EGFR), which is associated with aggressive behavior, poor prognosis, and lack of response to conventional hormonal or HER2-targeted therapies (doi.org/10.1038/s41598-020-63310-2). Large-scale transcriptomic and immunohistochemical studies have shown that EGFR is significantly upregulated in basal-like and TNBC subtypes. This signifies EGFR as a clinically relevant and druggable target (doi:10.30699/ijp.2025.2042447.3363).

EGFR-driven signaling in TNBC primarily depends on aberrant activation of its tyrosine kinase domain, which governs downstream proliferative and survival pathways. In this study, the EGFR crystal structure PDB ID: 4HJO, obtained from the Protein Data Bank, was selected because it represents the active kinase domain of EGFR in complex with a small-molecule inhibitor erlotinib, thereby accurately capturing the conformational and functional state for kinase inhibition. This structure provides a biologically and therapeutically valid binding site, enabling investigation of EGFR-targeted inhibitors in TNBC.

Computational techniques such as molecular docking and molecular dynamics simulations are increasingly used to predict protein-ligand interactions [4] accurately. Molecular docking generates three-dimensional models of protein-ligand complexes to predict ligand-binding affinities and modes of interaction with target proteins. This method supports the logical design of new medications by identifying active binding sites and assessing ligand conformations using energy scoring [5]. Docking algorithms are useful tools for preliminary research and drug discovery because they identify optimal binding modes by ranking ligand poses and minimizing system free energy [6]. Using an umbrella framework of the physics governing interatomic interactions, molecular dynamics (MD) simulations predict the motion of each atom in a protein or other molecular structure over time [7]. These computer models can reveal the

locations of every atom on femtosecond timescales while capturing a wide range of vital biomolecular processes, such as conformational change, ligand binding, and protein folding. Crucially, these modeling techniques can also forecast the atomic-level reactions of proteins to modifications such as mutations, phosphorylation, protonation, or ligand addition or deletion [8].

MATERIALS AND METHODS

Molecular docking

Molecular docking studies were performed using the Schrödinger Maestro software version to examine the interactions between newly designed quinoxaline derivatives (1–10) and the EGFR tyrosine kinase domain with erlotinib (PDB ID: 4HJO, respectively). The study also examined the interactions of the standard drug Erlotinib with the same receptor. This study's primary goal was to comprehend the molecular mechanisms underlying these substances' binding to the EGFR receptor. This would provide important details on their binding styles and potential applications as medicinal substances. LigPrep was used to prepare the ligands for the molecular docking study. LigPrep uses the Build Panel to generate 3D ligand representations and optimizes ligand structures for docking simulations.

The crystallographic structures of receptors were obtained from the Protein Data Bank, allowing us to perform protein docking. Specifically, we retrieved the structure with PDB ID 4hjo (the EGFR tyrosine kinase domain bound to erlotinib). The Protein Preparation Wizard was used to prepare these structures for the docking investigation. To create a clean and appropriate environment for the docking simulations, the preparation steps included adding hydrogen atoms and removing solvent molecules. In cases where the protein structures had bound ligands, such as Erlotinib, additional steps were taken to ensure accurate simulation of ligand-binding interactions and to assess binding affinities. The protein-ligand complexes were minimized to ensure that the bound ligands were in energetically favorable conformations within the protein binding site. Molecular docking was performed by referencing the cocrystallized bound ligands. These grids helped define the potential binding sites within the catalytic sites of the target proteins (e.g., the EGFR tyrosine kinase domain with erlotinib), which was crucial for guiding the docking simulations [9, 10]. To enable precise targeting of the ATP-binding pocket of EGFR, a receptor grid was created for docking calculations by centering the grid on the binding site of the co-crystallized ligand (erlotinib). To cover all important residues in the active site, the grid box dimensions were set to 40 Å × 40 Å × 40 Å. The centroid of the co-crystallized ligand inside the EGFR binding pocket was represented by the grid center coordinates, which were defined as

X = –10.45 Å, Y = 23.62 Å, and Z = 56.18 Å.

As part of the validation process for the docking protocol, Erlotinib was redocked into the proteins' catalytic sites. The successful occupation of similar binding pockets by these reference ligands, as seen in the crystallographic structures, further supports the accuracy of the docking methodology.

The molecular docking simulations employed the Glide Extra Precision (XP) mode, known for its high accuracy in predicting ligand binding poses and affinities. The docking process involved compounds 1-10 and Erlotinib. For each molecule, the docking simulations generated and saved three potential binding poses, utilizing the XP mode. This approach enabled exploration of different orientations and conformations of the ligands within the binding sites, helping identify the most energetically favorable binding modes. It has been shown that this approach is useful for predicting how small-molecule inhibitors bind to their target proteins [11]. The ligand design strategy is illustrated in Figure 1.

Drug likeness and synthetic accessibility evaluation

The drug-likeness and synthetic accessibility of the designed compounds were evaluated using the SwissADME web tool. Critical physicochemical parameters such as molecular weight, number of hydrogen-bond donors and acceptors, and lipophilicity (log P) were determined; all were consistent with Lipinski's rule of five, suggesting favorable oral bioavailability. Additional drug-like filters, including Veber's rule, Pan-assay interference compounds (PAINS) alerts, bioavailability scores, and synthetic accessibility indices, were also determined.

These parameters collectively provided a multidimensional assessment of the compounds' pharmacokinetic behavior, structural alert liability, and synthetic feasibility, supporting their potential as good drug candidates. The Swiss-ADME bioavailability radar provides a quick, easy visual check to see whether compounds have the right properties to be good drugs. The radar involves six key parameters: solubility (log S ≤ 6), saturation (fraction of sp^3-hybridized carbons ≥ 0.25), flexibility

(≤9 rotatable bonds), size (molecular weight between 150–500 g/mol), polarity [total polar surface area (TPSA) between 20 and 130 $Å^2$], and lipophilicity (XLOGP3 within −0.7 to +5.0). Compounds that fall inside the pink area are likely to have good bioavailability. Moreover, blood–brain barrier (BBB) permeability and passive GI absorption (human intestinal absorption) were determined using the BOILED-Egg model, which leverages a bidimensional representation based on Wildman and Crippen LogP (WLOGP) (computationally predicted lipophilicity value) and TPSA. According to this model, compounds in the yellow region (yolk) are likely to reach the brain. In contrast, those in the white region are likely to exhibit efficient passive absorption via the gastrointestinal tract [12].

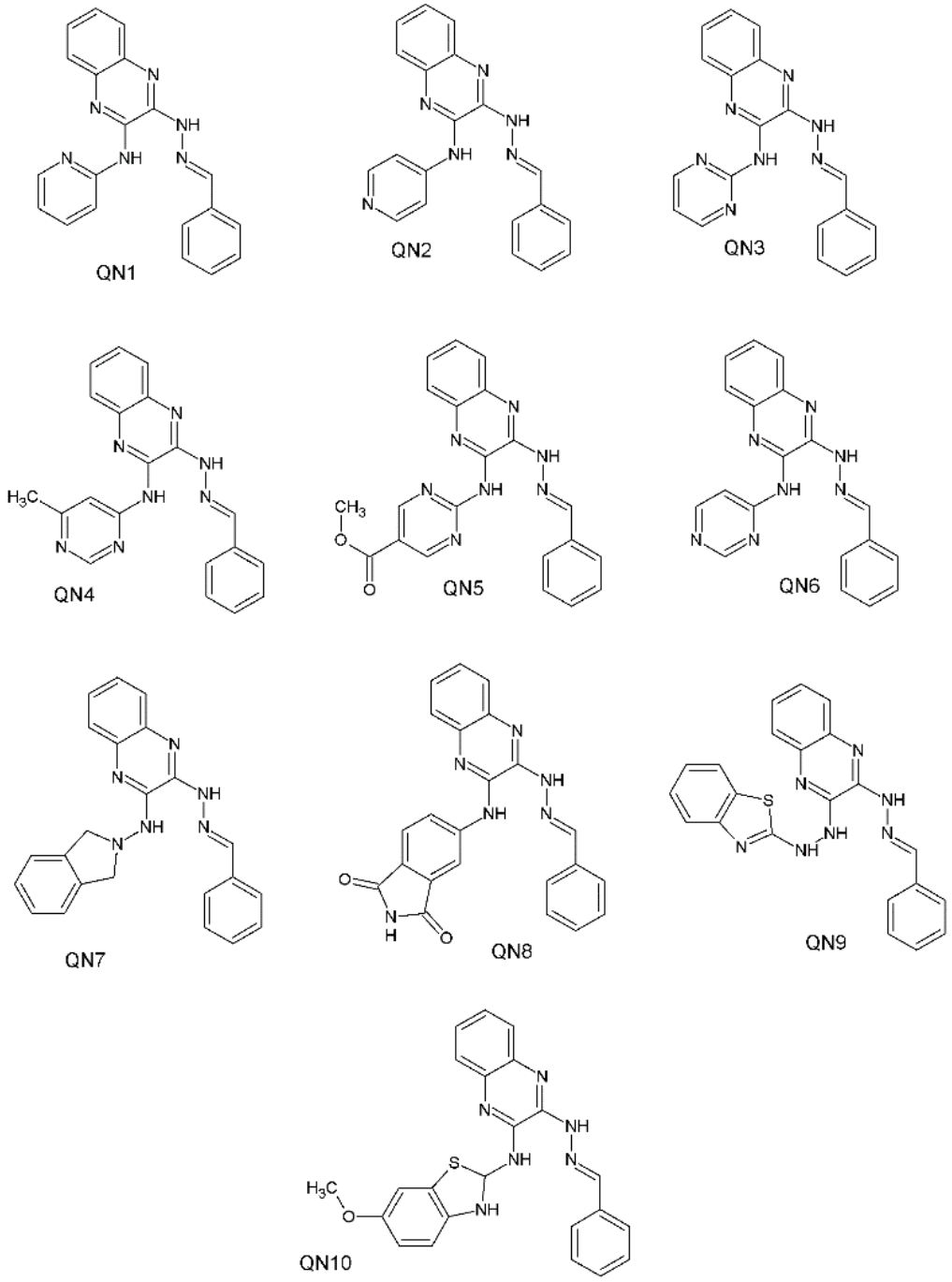

Figure 1: Designed amino quinoxaline derivatives (QN1–QN10)

ADMET study

In this study, the pkCSM web tool was utilized to predict the ADMET profiles of the designed compounds. The pkCSM platform utilizes graph-based structural signatures, which encode atomic distance relationships within compounds, to develop and refine robust predictive models. Detailed

pharmacokinetic and toxicity parameters were generated for each compound by using this tool. Key descriptors analyzed included intestinal absorption, BBB permeability, central nervous system (CNS) penetration, and skin permeation.

In addition, physicochemical properties such as TPSA and the number of rotatable bonds were determined to evaluate their influence on drug-likeness and pharmacokinetic performance. The comprehensive *in silico* analysis revealed that most compounds exhibited favorable ADMET characteristics, thereby reinforcing their suitability for further preclinical development [13].

MD simulations

Molecular dynamics (MD) simulation is widely regarded as an essential technique for understanding the dynamic behavior of protein–ligand interactions. An MD simulation production run of 100 ns was performed for each complex. GROMACS 2021.1 was used to run the MD simulation under a Linux operating system. The macromolecular system was meticulously set up before the production run. The CHARMM36 force field was used to construct the protein topology, and the SwissParam online service (SwissParam, 2011 release) was used to generate the ligand topology and parameters to ensure compliance with the CHARMM force field.

Throughout the simulation, a constant temperature of 300 K, a constant pressure of 1 atm, and a time step of 2 fs were all maintained. The TIP3P water model was used to solvate the system after each protein–ligand combination was placed in a cubic simulation box, with a minimum of 10 Å between the protein and the box edge. The necessary Na^+/Cl^- counter ions were then added to neutralize the system. The steepest-descent approach was used to minimize the energy of each system, thereby removing steric conflicts and closing atomic contacts.

The systems were then equilibrated in two stages, each for 5 ns: NVT ensemble (constant particle number, volume, and temperature) and NPT ensemble (constant particle number, pressure, and temperature). Subsequently, a 100 ns production MD simulation was run for trajectory analysis. The complexes' dynamic behavior and structural stability were assessed using metrics such as radius of gyration (Rg), root-mean-square deviation (RMSD), and root-mean-square fluctuation (RMSF). Additionally, binding free energy calculations were carried out using the gmx_MMPBSA program and the molecular mechanics generalized Born surface area (MM-GBSA) technique based on the MD simulation trajectories [14-16].

MMGBSA Analysis

To ascertain the compound's affinity for the receptors, an MM-GBSA analysis was performed on both the protein-ligand and complex systems. The 100 ns-long MDS trajectories were subjected to binding free-energy calculations using MM-GBSA. The binding energies determined using this method are more effective than the glide score values for choosing protein-ligand complexes.

The computation of MM-GBSA-based relative binding affinity is aided by the primary energy components, such as the H-bond interaction energy (DG Bind_Hbond), electrostatic solvation free energy (DG Bind_Solv), Coulomb or electrostatics interaction energy (DG Bind_Coul), lipophilic interaction energy (DG Bind_Lipo), and van der Waals interaction energy (DG Bind_vdW) [17].

RESULTS AND DISCUSSION

Molecular docking analysis

The in silico molecular docking method enhances the efficiency of drug discovery and reduces experimental costs and time. The Schrödinger Maestro suite (version 12.8, Schrödinger LLC, New York, USA) was used for all docking studies. The PROCHECK service was used to assess the structural quality of the EGFR tyrosine kinase receptor (PDB ID: 4HJO) using Ramachandran plot analysis before molecular docking. This analysis assesses the stereochemical quality of the protein backbone by examining the φ and ψ torsion angles of amino acid residues. The findings are demonstrated in the figure. 2. says that the receptor structure employed for docking experiments had good stereochemical quality, with 90.2% of residues found in the most favored regions, 8.7% in additionally allowed regions, 0.8% in liberally allowed regions, and 0.3% in disallowed regions.

The protein EGFR is bound by Erlotinib (AQ4), a competitive, reversible inhibitor of ATP. Erlotinib establishes one or more crucial H-bonds with the EGFR hinge region, usually with the residue Met793 in EGFR. Erlotinib's quinazoline ring slides into the ATP site's hydrophobic cleft. Residues such as Leu718, Val726, and Ala743 interact with the aromatic rings. Sensitivity versus resistance is significantly influenced by Thr790 (the T790M mutation results in resistance) [18].

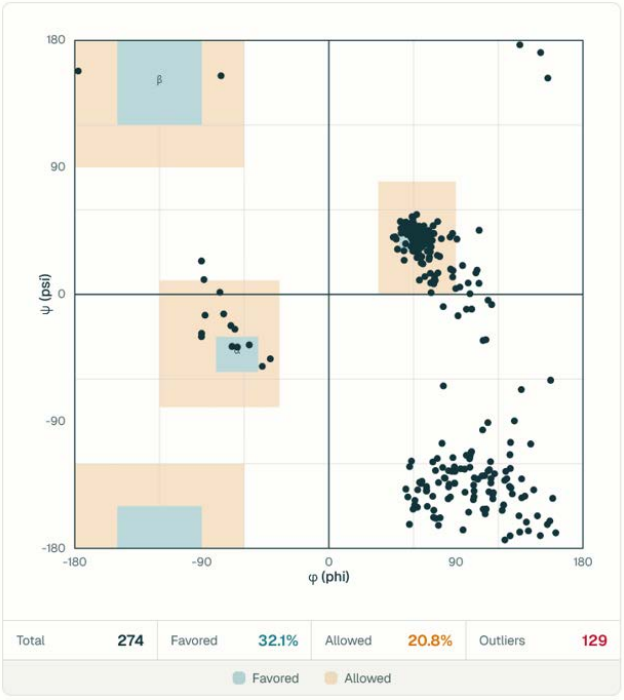

Figure 2: The Ramachandran plot for EGFR tyrosine kinase (PDB ID: 4HJO)

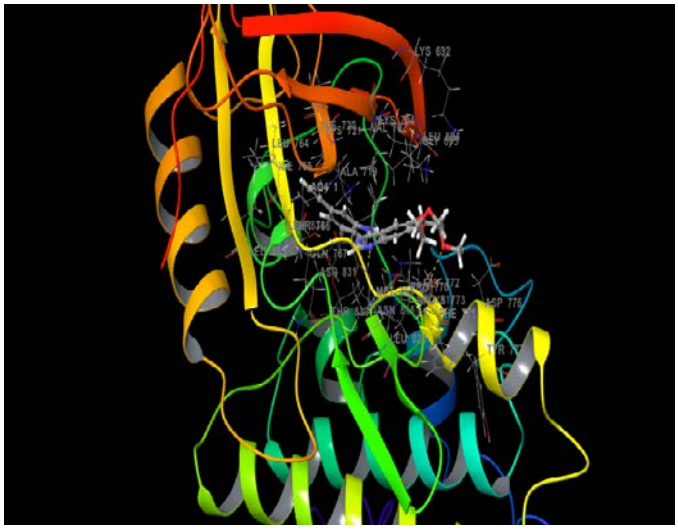

Figure 3: Redocking pose of the co- crystallized ligand AQ4(Erlotinib)

The binding mode of erlotinib provides a guide to the binding sites for novel ligand interactions, such as hydrogen bonds with Met769 (or similar residues in mutants), which are ideal for a strong EGFR inhibitor. Figure. 3 shows the Erlotinib (AQ4) interaction with the receptor EGFR (pdb 4HJO). Enhancing binding affinity involves filling the hydrophobic areas next to the hinge. Some ligands increase solubility and selectivity by extending into the solvent front. To overcome resistance, ligands must be designed to avoid steric clashes at Thr790 (or the T790M mutation). Erlotinib exhibits important pharmacophoric characteristics that guide the design of new ligands, such as hydrophobic/aromatic regions and H-bond donor/acceptor groups at the hinge. Next-generation drug design (e.g., Osimertinib) is aided by understanding the interactions between erlotinib and mutations that may disrupt binding [19-20]. For the current molecular docking study, the epidermal growth factor receptor (EGFR) crystal structure with PDB ID 4HJO was selected based on structural and pharmacological factors. 4HJO is an excellent choice for structure-based drug design, as it depicts the EGFR tyrosine kinase domain in complex with the clinically proven inhibitor Erlotinib (co-crystallized ligand AQ4).

A well-defined ATP-binding pocket is established by the presence of a bound ligand, enabling reliable validation of docking protocols through redocking studies and accurate identification of key interacting residues. The structure's excellent crystallographic resolution (~2.6 Å) provides reliable docking simulations and good atomic detail. Additionally, structural validation using PROCHECK (Ramachandran plot) confirmed that the protein possesses excellent stereochemical quality, with the majority of residues located in favored regions. The chosen structure matches EGFR's active conformation, which is especially important for developing ATP-competitive inhibitors such as the synthetic amino quinoxaline derivatives (QN1–QN10). Important residues in the hydrophobic pocket (Leu718, Val726, Ala743) and hinge region (e.g., Met793) that are necessary for ligand binding are oriented correctly in the active conformation. 4HJO shows a few missing residues in the binding site, guaranteeing that structural gaps or uncertainty in important interaction regions won't have a major impact on the docking results. A redocking analysis of the co-crystallized ligand (erlotinib) was carried out to verify the docking procedure. The precision and dependability of the docking technique employed in this investigation were confirmed by the overlaid pose of the redocked ligand with the crystallographic conformation, which showed good alignment (low RMSD).

Redocking for validation and grid generation

The co-crystallized ligand attached to the protein structure in the binding pocket was removed and redocked in the active site. This showed that the important interactions with key amino acid residues of the protein were correctly repeated. The redocking pose of the co- crystallized ligand AQ4(Erlotinib) is depicted in Figure 3. With inner grid box dimensions of 10 × 10 × 10 Å and

outer dimensions of 20 × 20 × 20 Å to suitably include the active site and allow ligand flexibility, the receptor grid was created using the Glide module by centering on the co-crystallized ligand. The precision and dependability of the docking setup were confirmed by re-docking the native ligand (erlotinib), yielding an RMSD of less than 2.0 Å. To accommodate for slight receptor flexibility, Van der Waals scaling was applied to receptor nonpolar atoms with a scaling factor of 0.8 and a partial charge cutoff of 0.15. The LigPrep module was used to create ligands, and flexible ligand sampling was enabled to facilitate comprehensive conformational research. The Glide Extra Precision (XP) mode, which uses a sophisticated scoring function that incorporates hydrophobic, electrostatic, and desolvation contributions, was used for docking. The final pose selection was based on the lowest Glide score, beneficial binding interactions (such as hydrogen bonding and π–π interactions with important active site residues), and consistency with the binding orientation of the co-crystallized ligand, even though each ligand produced three poses. Furthermore, ligand-protein interactions were refined, and the binding geometry was optimized through post-docking reduction using the OPLS-5 force field.

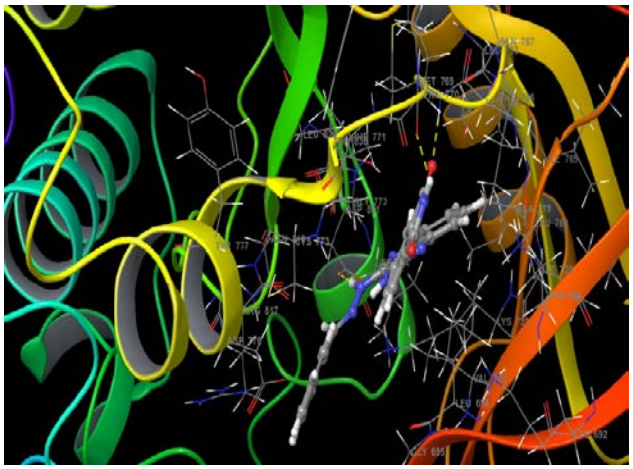

Figure 4: Docking pose of the designed ligand QN8

Post-docking analysis

The resulting docking poses were carefully examined, and those illustrating the most favorable ligand–receptor interactions were selected for further analysis. Among the ten designed series, four QN series compounds exhibited the highest binding affinities to the target protein. The binding affinities of "QN" series compounds ranged from −9.305 to −4.772 kcal/mol. And the docking process yielded a binding affinity score of −9.305 kcal/mol for QN8, as depicted in the figure. 4, which supports the new pose closely, matched the original one. Each selected compound underwent a detailed interaction analysis using the PLIP web server and PyMOL molecular visualization software, and the results were compared with the co-crystallized ligand (erlotinib).

Table 1: Docking Score and interactions between the top 4 compounds and AQ4

Compound	Binding affinity	Hydrogen bonding	π-stacking	Halogen bond
QN8	−9.30	MET 769, ASP 831	-	-
QN4	−8.728	MET 769, ASP 831	-	-
QN2	−8.063	MET 769, ASP 831	-	-
QN6	−8.031	MET 769, LYS 721	-	-
Co-crystallized ligand (Erlotinib)	**-9.501**	MET 769, CYS 773	-	-

The binding affinities and corresponding interaction profiles of these top four compounds and the co-crystallized ligand are summarized in Table 1. A mixture of important non-covalent interactions inside the EGFR active site is responsible for the lead chemical QN8's high binding affinity (−9.305 kcal/mol), according to the post-docking study. To anchor ATP-competitive inhibitors and replicate the interaction pattern of well-known medications such as Erlotinib and Osimertinib, QN8 forms an essential hydrogen bond with MET769, a hinge-region residue. Furthermore, the observed interaction with ASP831, located near the activation loop, suggests an extended binding mode that enhances both affinity and specificity and helps stabilize the ligand within the binding pocket. A mixture of important non-covalent interactions inside the EGFR active site is responsible for the lead chemical QN8's high binding affinity (−9.305 kcal/mol), according to the post-docking study. To anchor ATP-competitive inhibitors and replicate the interaction pattern of well-known medications such as Erlotinib and Osimertinib, QN8 forms an essential hydrogen bond with MET769, a hinge-region residue. Furthermore, the observed interaction with ASP831, located near the activation loop, suggests an extended binding mode that enhances both affinity and specificity and helps stabilize the ligand within the binding pocket. In addition to hydrogen bonding, QN8's quinoxaline scaffold and aromatic substituents are ideally positioned within the ATP-binding site's hydrophobic cleft, enabling substantial hydrophobic and van der Waals interactions with residues such as Leu718, Val726, and Ala743. The total binding energy and ligand-receptor complementarity are known to be significantly influenced by these interactions. Additionally, QN8's structural orientation appears to avoid steric clashes with the gatekeeper residue Thr790, which is frequently associated with resistance

mutations, suggesting a potentially advantageous binding profile. Strong hinge-region anchoring, additional stabilizing interactions, and numerous hydrophobic contacts collectively explain QN8's improved docking performance and bolster its potential as an effective EGFR inhibitor. The top-selected compounds exhibited significant hydrogen-bonding interactions with MET 769, ASP 831, and LYS 721. The co-crystallized ligand exhibited hydrogen bonding interactions with MET 769 and CYS 773. The interactions of the top 4 compounds and the co-crystal ligand at the binding site of the receptor are shown in Figure 5.

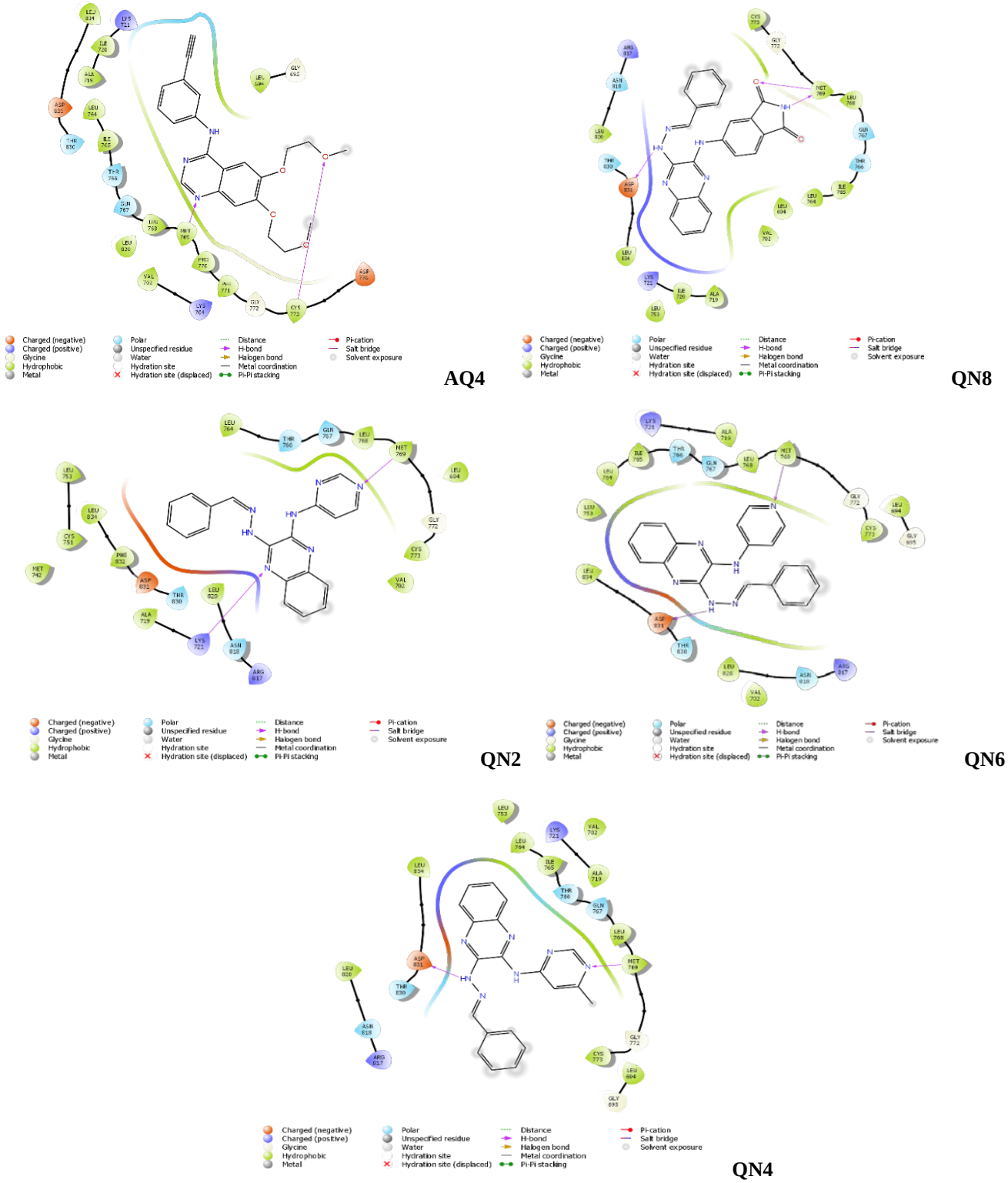

Figure 5: The interactions of the top 4 compounds and the co-crystal ligand with amino acids.

Evaluation of drug-likeness and synthetic accessibility

Numerous studies have demonstrated that the toxicological profiles and adverse effects of anticancer agents are closely correlated with their molecular weight and inherent chemical characteristics. In light of this, we conducted a detailed study of pharmacokinetic parameters and key characteristics of the designed derivatives, using the SwissADME web server to assess chemical properties and ADME profiles. The results are depicted in Table 2. The selected compounds and the standard drug Erlotinib satisfied Lipinski's rule of five. In addition, their predicted oral bioavailability was considered moderate, with an Abbott bioavailability score of 0.55. From a medicinal chemistry perspective, the compounds did not trigger alerts in the PAINS filters. The synthetic accessibility scores of the compounds ranged from 3 to 5, indicating moderate synthetic feasibility. While synthesis may require careful planning, it remains practical and acceptable for early-stage drug development. Overall, the compounds demonstrated favorable druggability, meeting Lipinski's rule of five, showing promising oral absorptivity, and demonstrating synthetic accessibility. These factors demonstrate their potential as chemotherapeutic agents or drug leads [21-22].

Table 2: Drug-likeness and synthetic accessibility assessment of selected compounds.

Compounds	QN 1	QN 2	QN 3	QN 4	QN 5	QN 6	QN 7	QN 8	QN 9	QN 10	Co-crystal ligand (Erlotinib)
Molecular weight (g/mol)	340.38	340.38	341.37	355.40	399.41	341.37	380.45	408.41	411.48	428.51	393.44
Hydrogen bond donors	2	2	2	2	2	2	2	2	3	3	1
Hydrogen bond acceptors	4	4	5	5	7	5	4	4	4	4	6
LogP	2.98	2.57	2.36	2.18	1.85	2.36	3.77	2.98	3.83	3.37	3.48
TPSA (Å²)	75.09	75.09	87.98	87.98	114.28	87.98	65.44	75.09	115.36	108.76	74.73
Rotatable bonds	5	5	5	5	7	5	5	5	6	6	10
Lipinski's rule of 5 violations	0	0	0	0	0	0	0	0	0	0	0
Veber's rule violations	0	0	0	0	0	0	0	0	0	0	0
Synthetic accessibility	3.44	3.38	3.22	3.39	3.36	3.31	3.52	3.44	3.71	4.42	3.19
Bioavailability score	0.55	0.55	0.55	0.55	0.55	0.55	0.55	0.55	0.55	0.55	0.55

ADMET study

The ADMET profiles of the designed compounds were comprehensively evaluated to assess their potential as therapeutic agents, with the corresponding data compiled in Table 3. All compounds demonstrated high predicted gastrointestinal absorption, indicative of efficient oral uptake, while concurrently exhibiting limited potential for CNS distribution. In the context of BBB permeability, a Log PS (permeability-surface area product) generally indicates significant CNS penetration. As CYP enzymes are implicated in the biotransformation of approximately 50% of clinically used drugs, their inhibition can lead to adverse drug–drug interactions and altered pharmacokinetics.

All the compounds show inhibitory activity against CYP1A2, CYP2C19, CYP2C9, CYP2D6, and CYP3A4, indicating potential for drug–drug interactions. However, this metabolic profile aligns with Erlotinib, a clinically approved EGFR tyrosine kinase inhibitor, suggesting that the risk of interaction is acceptable and manageable in the context of drug development. Nevertheless, the observed CYP450 inhibition highlights the need for further investigation during later development stages to assess & mitigate potential drug–drug interaction risks [23-24]. In addition to the core pharmacokinetic advantages, compound **QN8** was assessed using advanced drug-likeness metrics from SwissADME. The bioavailability radar (Fig. 6) confirmed that **QN8** aligns well with the optimal physicochemical space for oral drug candidates in terms of lipophilicity, molecular size, polarity, solubility, and flexibility; however, a deviation in the saturation parameter was noted, reflecting a reduced fraction of sp^3-hybridized carbons compared to the ideal threshold.

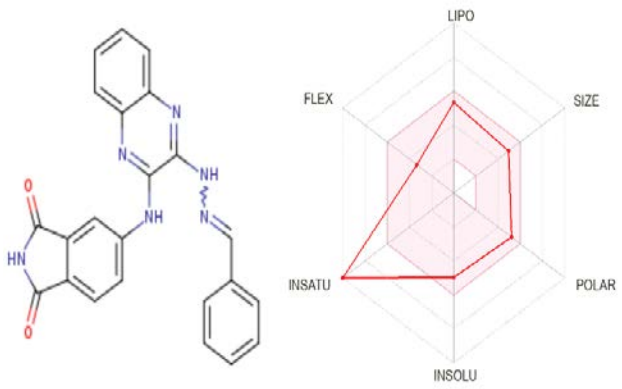

Figure 6: Bioavailability radar for QN8 showing physicochemical behavior

Table 3: Predicted ADMET parameters of selected compounds

Compounds	QN 1	QN 2	QN 3	QN 4	QN 5	QN 6	QN 7	QN 8	QN 9	QN 10	Co-crystal ligand (Erlotinib)
GI absorption	High	High	High	High	High	High	High	High	High	High	High
BBB permeation	Yes	Yes	No	No	No	No	Yes	No	No	No	Yes
P-gp substrate	No	No	No	No	No	No	Yes	No	No	No	No
CYP1A2 inhibitor	Yes	Yes	Yes	Yes	Yes	Yes	Yes	Yes	Yes	No	Yes
CYP2C19 inhibitor	Yes	Yes	Yes	Yes	Yes	Yes	Yes	Yes	Yes	Yes	Yes
CYP2C9 inhibitor	Yes	Yes	Yes	Yes	Yes	No	Yes	Yes	Yes	Yes	Yes
CYP2D6 inhibitor	Yes	Yes	Yes	Yes	Yes	Yes	Yes	No	Yes	Yes	Yes
CYP3A4 inhibitor	Yes	Yes	Yes	Yes	Yes	No	Yes	Yes	No	Yes	Yes
Log K_p (Skin permeation cm/s)	-5.32	-5.56	-5.79	-5.59	-6.25	-5.79	-5.23	-6.07	-4.45	-4.89	-6.35

Furthermore, the compound was evaluated using the BOILED-Egg model (Fig. 7), where it was located within the white region of the WLOGP versus TPSA plot. This region is associated with a high probability of passive gastrointestinal absorption, suggesting effective oral uptake. Such a positioning reflects a well-balanced lipophilic–polar profile, a crucial factor in membrane permeability, and reinforces the compound's suitability for oral administration and systemic bioavailability.

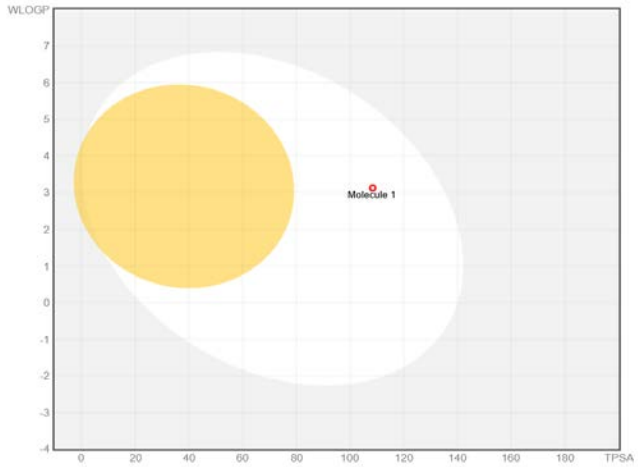

Figure 7: Boiled egg representations for QN8 showing physicochemical behavior

MD simulation

MD simulation is a powerful computational technique extensively used to explore the dynamic and structural properties of protein–ligand complexes. Due to its excellent profile, QN8 was selected for in-depth investigation using MD simulation. A 100-ns simulation was conducted to evaluate the stability and interaction dynamics of the compound QN8-EGFR-tyrosine kinase complex. For comparative purposes, the co-crystallized ligand of EGFR was subjected to identical simulation conditions. This strategy enabled a thorough comparison of QN8's dynamic behavior with that of the standard ligand, reinforcing its potential as a safe and effective lead compound. Key parameters, such as RMSD, RMSF, intermolecular hydrogen bonds, Ligand-protein contacts, and Ligand torsion profiles, were extracted from the simulation trajectories [25].

RMSD profile analysis

To assess the conformational and binding stability of the protein–ligand complexes, the RMSD of the protein backbone was calculated from the MD simulation trajectory. A higher backbone RMSD typically reflects conformational rearrangements, whereas a lower value suggests greater structural stability. A stable RMSD profile with minimal fluctuations indicates system equilibration. In this study, the EGFR-tyrosine kinase backbone RMSD for complexes with QN8 and the co-crystallized ligand was calculated and is shown in Figure 8. The average RMSD values for the co-crystal ligand, with both systems displaying consistent trajectories. Although the QN8 complex exhibited a slightly higher deviation, overall stability was maintained.

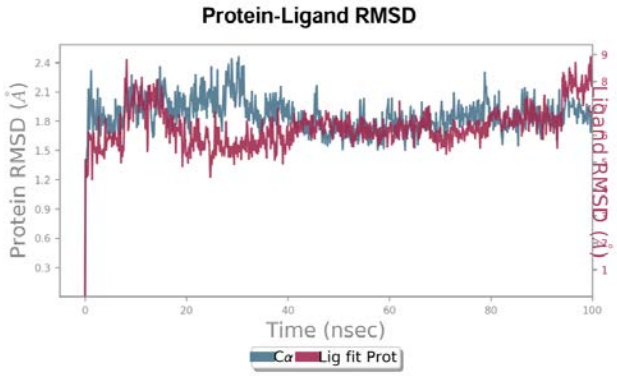

Figure 8: RMSD plot of the standard AQ4 and the co-crystallized ligand

Stability of the ligands during the simulation (Figure 9). The difference between the maximum and minimum RMSD for the co-crystal ligand indicates limited deviation from their initial binding poses. These findings indicate that both ligands maintained stable binding within the EGFR-tyrosine kinase active site throughout the simulation.

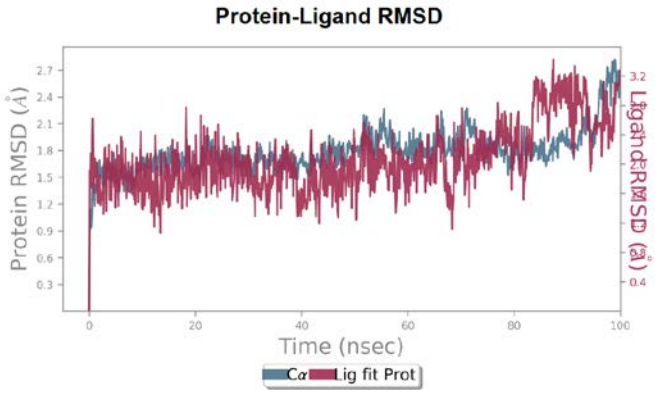

Figure 9: RMSD plot of the Compound QN8 and the co-crystallized ligand.

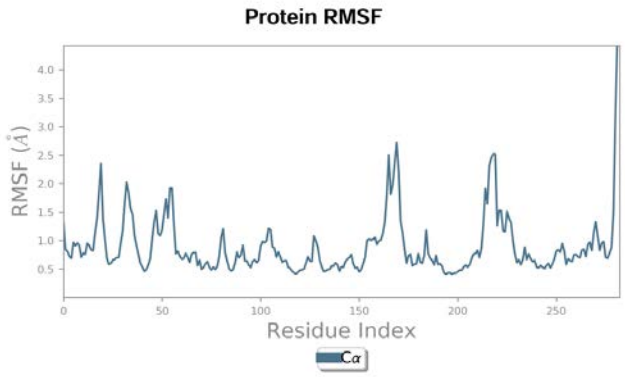

Figure 10: RMSF plot of the standard AQ4 and the co-crystallized ligand

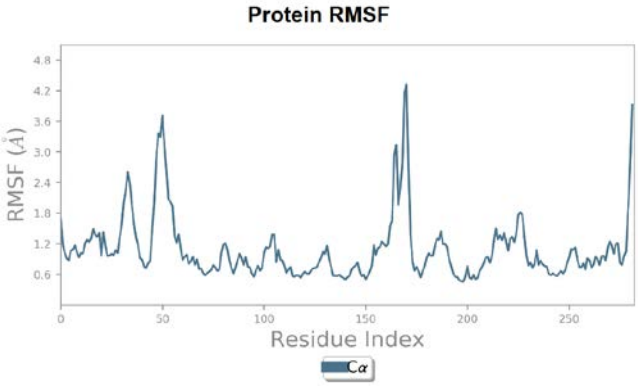

Figure 11: RMSF plot of the Compound QN8 and the co-crystallized ligand.

The EGFR–QN8 complex stabilized after reaching equilibration in the first 10–15 ns. The QN8 complex's average backbone RMSD was found to be roughly 2.1 ± 0.25 Å, while the co-crystallized ligand complex's average RMSD was 1.9 ± 0.20 Å, suggesting similar structural stability. The QN8-bound system exhibited somewhat greater deviations, but the fluctuations stayed within a reasonable range (1–3 Å), indicating that there was no significant conformational instability. Similar to the co-crystallized ligand, QN8 maintained a stable binding posture within the active site with little change from the initial conformation, according to the ligand RMSD study. These findings show that both systems reached equilibrium and maintained steady trajectories throughout the simulation.

Root-mean-square fluctuation

The RMSF, a key parameter for assessing the flexibility of individual amino acid residues, was systematically calculated for both complexes. These analyses offer valuable insights into the residue-level dynamics of the EGFR tyrosine kinase. Notably, while the catalytic region remained stable, certain residues exhibited greater fluctuations, reflecting a balance between structural rigidity and flexibility in the presence of standard Erlotinib (Figure 10) and QN8 (Figure 11).

Both complexes' average RMSF values fell between 1.0 and 2.5 Å, suggesting that the core catalytic domain has little flexibility. As is common in protein systems, loop regions and terminal residues showed the greatest variation. Crucially, in both complexes, key active-site residues showed little variation, indicating sustained ligand binding. The QN8 complex's fluctuation pattern resembled that of the reference ligand, indicating that the protein backbone was not significantly disrupted structurally by ligand binding.

Analysis of Hydrogen Bond Interactions

Analysis of protein–ligand interactions showed that QN8 consistently exhibited hydrophobic and hydrogen-bonding interactions throughout the simulation. Strong and enduring binding was indicated by hydrogen-bond occupancy in key interactions, which exceeded 60–70% of the simulation period. Significant contributions from hydrophobic contacts, π–π stacking, and water-mediated interactions, in addition to hydrogen bonds, helped maintain the ligand within the binding pocket.

SASA Analysis and the Radius of Gyration (Rg)

The compactness of the protein structure was assessed by tracking the radius of gyration (Rg). Throughout the simulation, the Rg values for both complexes stayed constant (~20–22 Å), suggesting no appreciable unfolding or structural expansion.

There were relatively minor variations in the solvent-accessible surface area (SASA) analysis, indicating that the protein's exposure profile to the solvent remained constant. During the simulation, the QN8 complex's structural stability was further supported by SASA values that were similar to those of the co-crystallized ligand.

Conformational Stability and Ligand Properties

Analysis was conducted on ligand-specific metrics, including molecular surface area, intramolecular hydrogen bonds, and torsion profiles. QN8 showed good adaptation within the binding pocket, exhibiting stable torsional behavior and minimal structural strain. Throughout the trajectory, the ligand's surface area and compactness remained constant, suggesting its stable binding configuration.

MMGBSA Analysis

The MMGBSA calculation showed that the designed compounds were most advantageous in terms of the sum of binding energies across different contributions, including lipophilic, Coulombic (electrostatic), and van der Waals. In contrast, the polar solvation energy (DG Bind sol_GB) decreased the binding free energy (DG Bind). The MMGBSA calculation showed that the system was most favorable in terms of the sum of binding energies across the lipophilic, Coulombic (electrostatic), and van der Waals contributions. In contrast, the polar solvation energy (DG Bind sol_GB) decreased the binding free energy (DG Bind). From the results, the large positive Coulomb energy observed for QN9 (+157.03 kcal/mol) does not indicate a simulation failure; rather, it reflects highly unfavorable electrostatic interactions that are compensated by solvation effects in the MM-GBSA framework. The Coulomb term represents the gas-phase electrostatic contribution, which can become strongly positive when charged or polar ligand groups interact electrostatically within the binding pocket. This coulomb energy is balanced by a strongly favorable polar solvation term (Ligand_Solv_GB = –77.13 kcal/mol) and stabilizing van der Waals and lipophilic interactions, resulting in an overall negative binding free energy (ΔG_bind = –66.23 kcal/mol). Trajectory analysis showed no abnormal RMSD fluctuations for the QN9 protein complex, supporting the reliability of the simulation. Therefore, the positive Coulomb energy reflects the electrostatic contribution and solvent stabilization. Also, the potent compounds QN8 (–9.305 kcal/mol) and Erlotinib (–9.501 kcal/mol) exhibit comparable docking scores; the larger energy gap observed in MM-GBSA calculations reflects methodological differences between the two approaches.

Docking scores provide a static, pose-based estimate of binding and key interactions. MM-GBSA evaluates binding free energy averaged over molecular dynamics trajectories, incorporating van der Waals, electrostatic, and solvation contributions. The more favorable MM-GBSA energy for Erlotinib indicates greater dynamic stability and stronger interaction networks within the EGFR binding pocket during simulation, whereas QN8, despite a favorable initial docking score, exhibits comparatively reduced energy under dynamic conditions. Thus, the MM-GBSA energy reflects differences in thermodynamic stability rather than docking pose quality. The MMGBSA values for the designed compounds are shown in Table 4.

Table 4: Calculated MMGBSA (kcal/mol) for the best docking-scoring ligands

Compound	MMGBSA _dG_Bind	MMGBSA _dG_Bind _Coulomb	MMGBSA _dG_Bind _Covalent	MMGBSA _dG_Bind _H bond	MMGBSA _dG_Bind _Lipo	MMGBSA _dG_Bind _vdW	Ligand _Solv_ GB	Prime_MM GBSA Liga nd_efficiency
AQ4	-97.2341	-29.5266	0.3828	-1.2464	-39.8731	-52.985	-7.3634	-5.0293
QN1	-74.9143	-15.6001	0.955519	-1.1497	-28.551	-51.3910	-8.1207	-4.0457
QN2	-74.9143	-15.6001	0.9555	-1.1497	-30.6252	-51.3911	-5.6095	-2.8813
QN3	-65.0519	-4.8062	2.1046	-0.1725	-29.7983	-50.1886	-7.6450	-3.753
QN4	-72.8239	-12.8848	-4.8796	-1.6134	-28.551	-51.8933	-8.1207	-2.6971
QN5	-67.4218	-14.5193	9.3784	-1.8672	-29.6668	-56.3318	-8.5523	-3.3710
QN6	-63.2826	-9.6143	2.6657	-1.3870	-29.6936	-50.0774	-5.7747	-2.4339
QN7	-69.775	-10.1292	4.889623	-1.0594	-34.4473	-51.0138	-4.6712	-3.6090
QN8	-73.6264	-22.1131	4.6612	-1.7308	-29.2425	-54.7072	-10.336	-2.3750
QN9	-66.2318	157.0313	3.912201	-1.9095	-27.7071	-52.4284	-77.125	-3.3115
QN10	-72.0685	-12.9587	1.071084	-3.3085	-30.8113	-55.4509	-5.5129	-3.4871

Structure-Activity Relationship

The 2nd position is known to affect the electronic distribution of the quinoxaline nucleus. This location allows substituents to alter electron density throughout the ring system, thereby indirectly affecting ligand–receptor interactions. Bulky substituents may provide steric hindrance close to the hinge area, while electron-withdrawing groups at this site may improve interaction with polar residues. The primary factor influencing biological activity was the 3-position. At this location, substituents directly engage in ligand–receptor interactions by extending into the ATP-binding pocket of the EGFR–tyrosine kinase domain.The observed activity trend (QN8 > QN6 > QN5 > QN3 > QN1) emphasizes the significance of:

- Hydrogen bond donor/acceptor capacity
- Aromatic π-system interactions (π–π stacking)
- Electronic complementarity with the binding pocket

QN8 (indole amine substitution) showed the most activity among the derivatives because multiple hydrogen-bond donors and acceptors increase the intensity of contact, a planar aromatic indole ring that makes it easier for active-site residues to stack π–π, and electron-donating characteristics that enhance electrostatic interactions. Simpler alkyl substitution (QN1), on the other hand, exhibited less activity because of its reduced hydrogen bonding capacity and lack of π-interactions.The fifth and sixth locations influence the binding pocket's steric alignment and hydrophobic interactions. Van der Waals interactions and binding affinity can be improved by adding small hydrophobic or halogen substituents at these locations. Solubility, pharmacokinetic characteristics, water-mediated interactions, and general molecular polarity are all known to be impacted by the 7th and 8th positions, which are usually oriented toward the solvent-accessible region. There were no replacements for positions 5, 6, 7, and 8 in the current study. Therefore, their implications are explained using existing SAR data instead of experimental observations from the current dataset. The overall SAR pattern of the newly designed quinoxaline derivatives is illustrated in Figure 12.

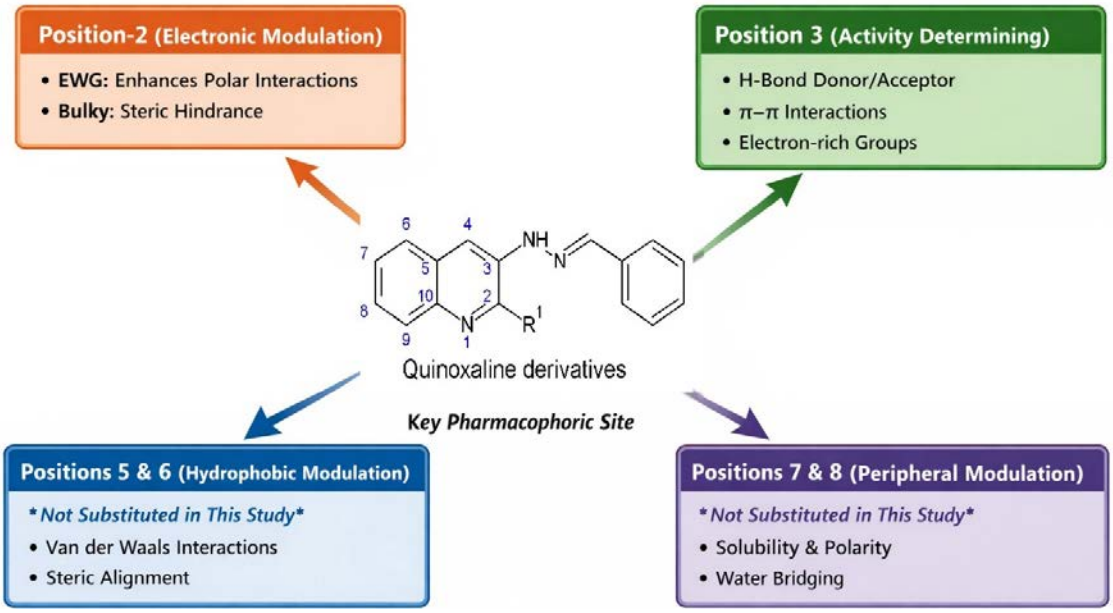

Figure 12: SAR for the newly designed compounds

Limitations of in silico research and prospects for the future

Although the current study uses molecular docking and molecular dynamics simulations to provide encouraging results for QN8 as a potential EGFR tyrosine kinase inhibitor, it is important to recognize several inherent limitations of these computational techniques. The full thermodynamic and kinetic characteristics of ligand-protein interactions may not always be accurately captured by molecular docking, which depends on simplified scoring functions that approximate binding affinity. These scoring functions may not accurately capture long-range electrostatic interactions and often ignore entropic contributions, leading to inaccurate rankings of ligand potency. In a similar vein, the precision of the applied force fields affects molecular dynamics simulations. Force fields such as CHARMM36 may not fully capture all atomic interactions, despite their widespread validation, especially for new molecular scaffolds like QN8. Furthermore, explicit or implicit water models that mimic physiological circumstances but might not accurately represent

the intricate cellular milieu are commonly used to describe solvent effects. The limited simulation timescale (100 ns) is another drawback, as it may miss uncommon binding/unbinding events or slower conformational changes. Moreover, biological factors such as protein expression levels, cellular absorption, metabolism, and off-target effects are not accounted for by computational models. As a result, even though the current in silico studies provide insights into the binding stability and interaction profile of QN8, they should be regarded as predictive rather than conclusive. To verify the compound's medicinal potential, experimental validation is crucial. To validate the computational predictions and evaluate the biological efficacy and safety of QN8, future research will focus on in vitro assays, including EGFR kinase inhibition assays and cell-based cytotoxicity studies.

CONCLUSION

The current study employed extensive in silico techniques, including molecular docking, molecular dynamics simulations, MM-GBSA analysis, and ADMET profiling, to design and assess a series of quinoxaline derivatives (QN1–QN10) targeting the EGFR tyrosine kinase. The findings showed that several drugs exhibited interaction patterns and binding affinities similar to those of the co-crystallized ligand erlotinib. Among these, QN8 showed a good binding profile with favorable hydrophobic contacts within the ATP-binding pocket, stable hydrogen bonding with important hinge area residues, and acceptable pharmacokinetic characteristics.

The structural stability of the QN8–EGFR complex during the simulation period was further confirmed by molecular dynamics simulations. It is crucial to remember that these results are based only on computational predictions and do not provide conclusive proof of biological function. As a result, QN8 shouldn't be regarded as a verified EGFR inhibitor as yet. Alternatively, it could be considered a computational lead molecule that shows promise and merits more research. To confirm its therapeutic potential and determine its efficacy and safety profile, more research incorporating synthesis, in vitro EGFR kinase inhibition tests, and cell-based assessments is required.

ACKNOWLEDGEMENTS

The authors are thankful to the D. E. Shaw Research Group and Schrödinger, Inc. for providing an academic-use version of the Desmond suite.

FINANCIAL ASSISTANCE

NIL

CONFLICT OF INTEREST

The authors declare no conflict of interest.

AUTHOR CONTRIBUTION

Abitha H contributed to the conception and design of the work and carried out the *in-silico* studies, including ADME prediction and molecular docking analysis. D. Kumudha critically reviewed, corrected, and substantively revised the manuscript for important intellectual content. Bhuvaneswari Sivaraman and M. K. Kathiravan performed the molecular dynamics (MD) simulation studies and contributed to the interpretation of the simulation data. All authors have approved the submitted version of the manuscript and any substantially modified version that involves their contribution to the study.

REFERENCES

[1] Jackson K, Nkoana A, Garland K, More K, et al. Synthesis and in vitro exploration of the 8-carbo substituted 5-methoxyflavones as anti-breast and anti-lung cancer agents targeting protein kinases (VEGFR-2 & EGFR). *Bioorg Chem*, **153**, 107875 (2024) https://doi.org/10.1016/j.bioorg.2024.107875

[2] Lehmann BD, Jovanović B, Chen X, et al. Refinement of triple-negative breast cancer molecular subtypes: implications for neoadjuvant chemotherapy selection. *PLoS One*, **11(6)**, e0157368 (2016) https://doi.org/10.1371/journal.pone.0157368

[3] Samantaray A, Pradhan D. Novel combination therapy of Osimertinib and Tupichinol E in triple-negative breast cancer: targeting EGFR and CDK4/6 pathways. *Aspects Mol Med*, **5**, 100069 (2025) https://doi.org/10.1016/j.amolm.2025.100069

[4] Herdiansyah MA, Ansori ANM, Kharisma VD, Maksimiuk MR, et al. In silico study of cladosporol and its acyl derivatives as anti-breast cancer agents against estrogen receptor-α. *Biosaintifika*, **16**, 142–154 (2024) https://doi.org/10.15294/biosaintifika.v15i1.949

[5] Trott O, Olson AJ. AutoDock Vina: improving the speed and accuracy of docking with a new scoring function. *J Comput Chem*, **31(2)**, 455–461 (2010) https://doi.org/10.1002/jcc.21334

[6] Muhammed MT, Aki-Yalcin E. Molecular docking: principles, advances, and its applications in drug discovery. *Lett Drug Des Discov*, **21(3)**, 480–495 (2024) https://doi.org/10.2174/1570180819666220922103109

[7] Karplus M, McCammon JA. Molecular dynamics simulations of biomolecules. *Nat Struct Biol*, **9**, 646–652 (2002) https://doi.org/10.1038/nsb0902-646

[8] Hollingsworth SA, Dror RO. Molecular dynamics simulation for all. *Neuron*, **99**, 1129–1143 (2018) https://doi.org/10.1016/j.neuron.2018.08.011

[9] Ejeh S, Otaru HA, Ejeh JE, John J, Ajala A, Omowanle J, et al. Computational techniques for analyzing quinoxaline-containing molecules as anti-schistosomal agents using docking, pharmacokinetics, drug-likeness, QSAR and molecular dynamics evaluation. *In Silico Res Biomed*, **1**, 100024 (2025) https://doi.org/10.1016/j.insi.2025.100024

[10] Badithapuram V, Nukala SK, Thirukovela NS, Dasari G, Manchal R, Bandari S. Design, synthesis, and molecular docking studies of quinoxaline derivatives as EGFR targeting agents. *Russ J Bioorg Chem*, **48(3)**, 565–575 (2022) https://doi.org/10.1134/S1068162022030220

[11] Salem MG, Abu El-Atab SA, Elsayed EH, Mali SN, Alshwyehde HA, Almaimani G, et al. Novel 2-substituted quinoxaline analogs with antiproliferative activity against breast cancer. *RSC Adv*, **13**, 33080–33095 (2023) https://doi.org/10.1039/D3RA06189B

[12] Saritha K, Alivelu M, Mohammad M. Drug-likeness analysis and in silico ADMET profiling of compounds in *Kedrostis foetidissima*. *In Silico Pharmacol*, **12(2)**, 67 (2024) https://doi.org/10.1007/s40203-024-00240-1

[13] Pires DEV, Blundell TL, Ascher DB. pkCSM: predicting small-molecule pharmacokinetic and toxicity properties using graph-based signatures. *J Med Chem*, **58(9)**, 4066–4072 (2015) https://doi.org/10.1021/acs.jmedchem.5b00104

[14] Kato K, Nakayoshi T, Kurimoto E, Oda A. Molecular dynamics simulations for protein–ligand complexes obtained by docking studies. *Chem Phys Lett*, **781**, 139022 (2021) https://doi.org/10.1016/j.cplett.2021.139022

[15] Pentu N, Azhakesan A, Kumar PK. Insilico molecular docking and ADME/T studies of flavonol compounds against selected proteins involved in inflammation mechanism. *J. Appl. Pharm. Res.*, **13**, 95–111 (2025) https://doi.org/10.69857/joapr.v13i1.706.

[16] Genheden S, Ryde U. MM/PBSA and MM/GBSA methods to estimate ligand-binding affinities. *Expert Opin Drug Discov*, **10(5)**, 449–461 (2015) https://doi.org/10.1517/17460441.2015.1032936

[17] Park JH, Liu Y, Lemmon MA, Radhakrishnan R. Erlotinib binds inactive and active conformations of EGFR tyrosine kinase domain. *Biochem J*, **448(3)**, 417–423 (2012) https://doi.org/10.1042/BJ20121513

[18] Wanode DM, Bhendarkar KP, Khedekar PB. Discovery of pyrazole–pyrazoline derivatives as VEGFR-2 kinase inhibitors: an in silico approach. *J Appl Pharm Sci*, **16(2)**, 122–135 (2025) https://doi.org/10.7324/JAPS.2026.256031

[19] Sharma VK, Nandekar PP, Sangamwar A, Pérez-Sánchez H, Agarwal SM. Structure-guided design and binding analysis of EGFR inhibiting analogues. *RSC Adv*, **6**, 105920–105939 (2016) https://doi.org/10.1039/C6RA20811C

[20] Mousavinejad SN. Molecular docking comparison of icotinib and erlotinib as EGFR inhibitors. *Zahedan J Res Med Sci*, **28(1)**, e165680 (2026) https://doi.org/10.5812/zjrms-165680

[21] Daina A, Michielin O, Zoete V. SwissADME: a free web tool to evaluate pharmacokinetics and drug-likeness of small molecules. *Sci Rep*, **7**, 42717 (2017) https://doi.org/10.1038/srep42717

[22] Bakchi B, Krishna AD, Sreecharan E, Ganesh VBJ, Niharika M, Maharshi S, et al. Applications of SwissADME web tool in medicinal chemistry. *J Mol Struct*, **1259**, 132712 (2022) https://doi.org/10.1016/j.molstruc.2022.132712

[23] Xu ZY, Li JL. Drug–drug interactions with EGFR tyrosine kinase inhibitors in NSCLC treatment. *Onco Targets Ther*, **12**, 5467–5484 (2019) https://doi.org/10.2147/OTT.S194870

[24] Kucharczuk CR, Ganetsky A, Vozniak JM. Drug–drug interactions, safety, and pharmacokinetics of EGFR tyrosine kinase inhibitors. *J Adv Pract Oncol*, **9(2)**, 189–200 (2018) https://doi.org/10.6004/jadpro.2018.9.2.5

[25] Shetty SR, Debnath S, Majumdar K, Rajagopalan M, Ramaswamy A, Das A. Virtual screening, molecular dynamics simulations, and in vitro validation of EGFR inhibitors as breast cancer therapeutics. *Bioorg Chem*, **153**, 107849 (2024) https://doi.org/10.1016/j.bioorg.2024.107849